# Melting of colloidal crystal in a two-dimensional periodic substrate: Switch from a single crossover to two-stage melting

Akhilesh M P\* and Toby Joseph<sup>†</sup>
Department of Physics, BITS-Pilani, K K Birla Goa Campus, Zuarinagar, Goa-403726, India
(Dated: October 2, 2025)

The melting transitions of a colloidal lattice confined to a two-dimensional (2D) periodic substrate of square symmetry are studied using Monte Carlo simulations. When the strengths of interparticle and particle-substrate interactions are comparable, the incommensurate nature of square and triangular ordering leads to the formation of a partially pinned solid with only one of the smallest G vectors of the substrate present. This low-temperature phase has true long-range order. By varying the lattice parameter of the substrate while keeping the filling fraction constant, it is seen that the transition from this low-temperature solid to a high-temperature modulated liquid phase can happen via either a single crossover transition or by a two-stage melting process. The transitions are found to be second-order in nature when the lattice parameter is  $d \lesssim 9\lambda$ , as confirmed by the finite-size scaling behavior of the specific heat. For the two-stage melting scenario, the intermediate phase is found to be hexatic. The transitions observed in this work are different from the predictions of the KTHNY theory. The study reveals how constraints from substrate periodicity can fundamentally alter melting dynamics, offering insights into the design of tunable colloidal systems and advancing the understanding of phase transitions in two-dimensional particle systems.

### I. INTRODUCTION

In 2D, understanding the rich interplay of order, fluctuations, and topology is crucial in predicting the phase behavior of solids under various system conditions. At finite temperatures, in the crystalline phase, the longwavelength fluctuations destroy the long-range positional order of the systems in 2D. Thus, no long-range positional order can exist in the 2D crystalline phase according to the Mermin-Wagner theorem [1]. A comprehensive theory of 2D melting based on topological defects was developed by Kosterlitz, Thouless, Halperin, Nelson, and Young, called KTHNY theory[2–6]. Several experimental [7-21], theoretical [22-27], and simulation studies [28–45] have been carried out to understand the melting transition of solids in 2D. Although some of the experimental results show conformity to the predictions of the KTHNY theory [7, 10, 12–15, 17–21], others differ in the number and nature of transitions

According to the KTHNY melting scenario, the transitions are mediated by two types of topological defects: dislocations and disclinations. A dislocation can be described by a pair of five-fold and seven-fold oriented sites, a disclination by an isolated five-fold or seven-fold oriented site in a triangular lattice structure. KTHNY melting scheme consists of two stages (i) a transition from a crystalline phase to an intermediate thermodynamic phase termed, hexatic phase mediated by unbinding of bound dislocations, and (ii) a transition from a hexatic phase to an isotropic liquid phase, mediated by unbinding of bound disclinations. In the crystalline phase, the system has quasi-long-range positional order and long-range

bond orientational order. But in the hexatic phase, the positional order is short-range, but retains a quasi-long-range orientational order. The existence of the hexatic phase has been confirmed in several experimental and simulation studies[11, 37, 46–50]. One of the key factors that determines whether the KTHNY scenario manifests is the core energy of the dislocation [24, 26, 27, 33]. It is observed that when the free dislocation core energy of the system is small (less than  $2.84\,k_BT$ ), then the system would follow the grain boundary melting that preempts the formation of the hexatic phase[51].

A related problem that has been of interest is the study of 2D particle systems in the presence of periodic substrates. The effect of the periodic substrate can crucially depend on the symmetry of the substrate as well as the commensurate or incommensurate nature of the substrate. In the presence of a periodic substrate with 1D modulation, the studies reveal that the system can undergo a freezing transition followed by a melting transition as the substrate strength is increased [52–55]. For periodic substrates with triangular symmetry, Nelson et al. have predicted the existence of a commensurate solid, a floating solid, and a modulated liquid depending upon commensuration between lattice and substrate as well as temperature [56]. In the weak substrate limit, the melting of a Xe monolayer adsorbed on Ag identifies the presence of a hexatic phase [57], which indicates the feature of 2D melting. The two-stage melting with the presence of an intermediate phase (with short-range positional order, but solid-like) has been observed in a monolayer of Ar adsorbed on a graphite substrate [58]. However, in an experimental study of an incommensurate monolayer of solid adsorbed on a 2D substrate, a single peak in the specific heat has been observed that corroborates a first-order phase transition in the system [59].

Studies have been carried out on 2D particle systems in periodic square symmetric substrates (the ratio of the

<sup>\*~</sup>p20210003@goa.bits-pilani.ac.in, akhileshmadathil@gmail.com

<sup>†</sup> toby@goa.bits-pilani.ac.in

number of particles to the number of substrate minima) [56, 60, 61]. Nelson et al. predicted that an Isinglike transition replaces the disclination unbinding transition in the usual KTHNY scenario of phase transition [56]. Using Monte-Carlo simulations, Toby et al. [61] have studied the phases and phase transition of the vortex lattice in a 2D periodic substrate of square symmetry when the strengths of the inter-vortex interaction and the vortex-substrate interactions are comparable. For a filling fraction (number of vortices per unit cell of square substrate) equal to one, a low-temperature partially pinned phase was observed. As the temperature is increased, this phase melts to a modulated square liquid via a second-order transition. A similar phase has been identified by T. Neuhaus et al. (referred to as the rhombic phase in that work), in a system of hard disks in a square symmetric substrate [60], by employing the Monte-Carlo simulation and density functional theory(DFT). For high substrate strength, a single secondorder transition is seen from the rhombic phase to the modulated phase as the packing fraction is decreased. At low substrate strengths, they find three separate phases with the rhombic phase giving way to triangular order at high packing fractions.

In the current work, we propose to study a system of colloidal particles interacting via a screened Coulomb potential in the presence of a square-symmetric potential for filling fraction equal to one. The key parameters concerning which we study the phases of the system are the size of the square substrate (relative to the screening length) and the strength of the substrate. Though the partially pinned solid and its continuous transition to a modulated liquid are found, like in the case of the vortex lattice study [61], a two-stage melting is observed as the size of the square substrate is decreased. Both these transitions are found to be second-order in nature, as confirmed by the finite-size scaling study of the specific heat.

This paper is organized as follows: In section II, we introduce the system, the simulation method used, and the details of the various quantities studied in the simulations. In section III, the results obtained from the study are presented, followed by a discussion of the results. In section IV, we conclude the work, discuss possible experimental avenues to explore, and discuss future directions.

## II. MODEL AND SIMULATION

The system that has been investigated encompasses a collection of  $N_p$  interstitial colloidal particles (referred to as particles henceforth) confined to move in a 2D periodic square symmetric substrate. The substrate is effected by the interaction of these interstitial colloidal particles with a fixed set of colloidal particles (referred to as pinned particles henceforth), located at the corners of a square lattice of sides d (see Fig.1). The interstitial particles

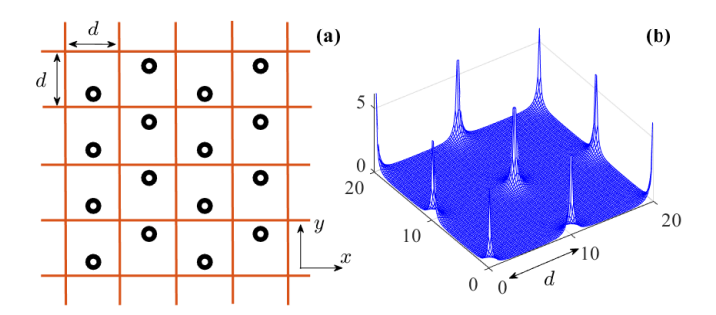


FIG. 1. (a) A schematic of the partially pinned structure of the colloidal lattice with the underlying substrate. The black circles represent the colloidal particles, and the red lines indicate the underlying square symmetric substrate with spacing d. The pinned colloidal particles are located at the corners of the squares (b) The potential landscape of the substrate formed by the pinned particles which interact with the interstitial ones via screened Coulomb interaction.

interact with each other by screened Coulomb interaction given by

$$U_i^{cc} = U_0 \sum_{\substack{j=1\\j \neq i}}^{N_p} \frac{e^{-\frac{r_{ij}}{\lambda}}}{r_{ij}} \tag{1}$$

where  $U_i^{cc}$  is the energy of the  $i^{th}$  particle due to the interaction between other particles in the lattice,  $r_{ij} = |\mathbf{r}_i - \mathbf{r}_j|$  is the interparticle separation,  $U_0$  is the strength of the interaction potential, and  $\lambda$  is the screening length of the potential. The interstitial particles also interact with the pinned particles via the same type of interaction, but with different interaction strength. The energy of the  $i^{th}$  particle in the lattice as a result of the interaction with the pinned particles of the substrate is given by

$$U_i^{cp} = A_s U_0 \sum_{\substack{k=1\\k\neq i}}^{N_p} \frac{e^{-\frac{r_{ik}}{\lambda}}}{r_{ik}}$$
 (2)

where  $A_s$  is a parameter that accounts for the effect of the strength of the substrate. The system is in contact with a thermal reservoir at temperature T. The Monte Carlo simulation technique that utilizes the Metropolis-Hastings algorithm is used to study the equilibrium phase behavior of the system. It is assumed that the pinned particles wouldn't be depinned from their respective pinned sites due to thermal fluctuations in the system. So the dynamics of these particles can be ignored in the simulations.

A thermodynamic quantity of interest in understanding the nature of the phase transition is the specific heat at constant volume  $C_v$ . It can be determined by the fluctuation in energy of the system by the relation

$$C_v = \frac{\langle (E - \langle E \rangle)^2 \rangle}{N_p k_B T^2} \tag{3}$$

where E is the total energy of the system and  $k_B$  is the Boltzmann constant. The low-temperature phase obtained in the study is a crystal with long-range positional order. To find out the translational(positional) symmetry breaking point, the global translational order parameter for the two smallest reciprocal lattice vectors  $\mathbf{G}_1$  and  $\mathbf{G}_2$  of the lattice is calculated using,

$$\Psi_T = \left| \frac{1}{N_p} \sum_{i=1}^{N_p} \psi_{T_i} \right| \tag{4}$$

where  $\psi_{T_i} = e^{i(\mathbf{G} \cdot \mathbf{r}_i)}$  is the local translational order parameter for the  $i^{th}$  particle at the position  $\mathbf{r}_i = (x, y)$ . The translational order parameter can give information about the structural change due to the change in position of the particle during melting. The static structure factor is computed using the vector  $\mathbf{q}$  in the reciprocal lattice space by

$$S(\mathbf{q}) = \frac{1}{N_p^2} \sum_{i,j} e^{i\mathbf{q}.(\mathbf{r}_i - \mathbf{r}_j)}$$
 (5)

To locate the point at which the orientational symmetry of the lattice breaks, the global orientational order parameter defined by,

$$\Psi_6 = \left| \frac{1}{N_p} \sum_{i=1}^{N_p} \psi_{6_i} \right| \tag{6}$$

is computed. Here  $\psi_{6_i} = \sum_{j=1}^{n_i} e^{i(6\theta_{ij})}/n_i$  is the local orientational order parameter for the  $i^{th}$  particle,  $\theta_{ij}$  is the angle between a bond formed by  $i^{th}$  and  $j^{th}$  particles and a reference axis, and  $n_i$  is the number of nearest neighbors of the  $i^{th}$  particle. The orientational order parameter gives information about the change in bond orientational order in the lattice.

To find the transition points accurately, the susceptibility is a useful quantity to study. It is defined as the fluctuation of the order parameter. This method would work well in identifying the transition points as it has less finite-size effects inherent in correlation functions[11]. The susceptibilities are given by

$$\chi_a = A(\langle \psi_a^2 \rangle - \langle \psi_a \rangle^2) \tag{7}$$

where A is the area of the system and the subscript a stands for T, 6.  $\chi_T$  measures the translational susceptibility and  $\chi_6$  measures the orientational susceptibility. The peak in susceptibility values can be used to accurately locate the transition points, both in simulation[38, 62] and in experiments[11, 63]. To characterize the different phases of the system, the orientational correlation function given by

$$g_6(\mathbf{r}) = \langle \psi_6^*(\mathbf{r}_i)\psi_6(\mathbf{r}_j)\rangle \tag{8}$$

has been calculated. Here,  $\psi_6(\mathbf{r})$  represents the local bond orientational order parameter of the particle at the position  $\mathbf{r}$ .

In simulation, the following units are used:  $\lambda = 1$  and  $k_BT$  in units of  $U_0 \frac{e^{-d/\lambda}}{d}$  with  $U_0 = 1$ . The average values of the various quantities in the study have been carried out over  $5 \times N_p \times 10^8$  Monte Carlo steps after allowing the system to equilibrate for  $N_p \times 10^5$  Monte Carlo steps. The simulated annealing technique has been used to obtain the low-temperature structure of the system. Additionally, it is ensured that the number of Monte Carlo steps is sufficient for the proper equilibration of the system. Though most of our simulations are carried out for  $L \times L$  system, we have ensured that the imposition of square boundaries does not have any influence on our results. This was done by verifying our results using a rectangular-shaped boundary that is commensurate with the triangular lattice for the same density. To understand the role of defect generation in the melting of the lattice, Voronoi-tessellation is performed. Using this technique, the distribution of topological defects: isolated dislocations, disclinations, and bound dislocations, in different phases is studied. Simulation studies are carried out for various system sizes to do finite-size scaling analysis.

# III. RESULTS AND DISCUSSION

The simulation studies have been carried out for filling fraction, n=1, by changing both the lattice spacing d and substrate strength,  $A_s$ . For  $d = 5\lambda$  and  $A_s = 10^{-4}$ , the low temperature phase is the partially pinned solid (rhombic structure) with an equal distance of separation  $\approx 0.13d$  from the minima on either side of the square cell, similar to the one observed in vortex lattice simulation [61] and for the hard sphere system [60]. Remarkably, a two-stage melting is observed in this case. The variation of  $C_v$  with temperature for this case is shown in Fig.2. Two distinct peaks, one at  $k_B T_{c1} = 0.07 U_1$  and the other at  $k_B T_{c2} = 0.25 U_1$  are seen, indicating the possible occurrence of two phase transitions. Here,  $U_1 = U_0 \frac{e^{-\delta}}{5\lambda}$ is the energy scale corresponding to the inter-particle interaction for the present case. Different system sizes  $(L \times L = 144, 196, 256, 400, 676, \text{ and } 900, L \text{ being the lin-}$ ear size of the system) were studied to ensure the robustness of the results and to check the presence of scaling. It has been observed that the peaks in  $C_v$  shift towards lower temperatures as the size of the system is increased. Two peaks in the  $C_v$  plot indicate the presence of an intermediate phase between the solid and the modulated liquid. The order parameters  $\Psi_{T_1}, \Psi_{T_2}$  and  $\Psi_6$  as well as the corresponding susceptibilities were computed (see Fig.3, 4) to gain insight into the nature of the phases involved. The translational and bond orientational orders drop smoothly around two different temperatures. Since the variations of  $\Psi_{T_1}, \Psi_{T_2}$  and  $\Psi_6$  with  $k_BT$  are inconclusive to locate the transition points, the susceptibilities of the order parameters have been computed. The corresponding susceptibilities show sharp peaks at two distinct temperatures, which are aligned with the location of the observed peaks in  $C_v$  at all system sizes studied. These

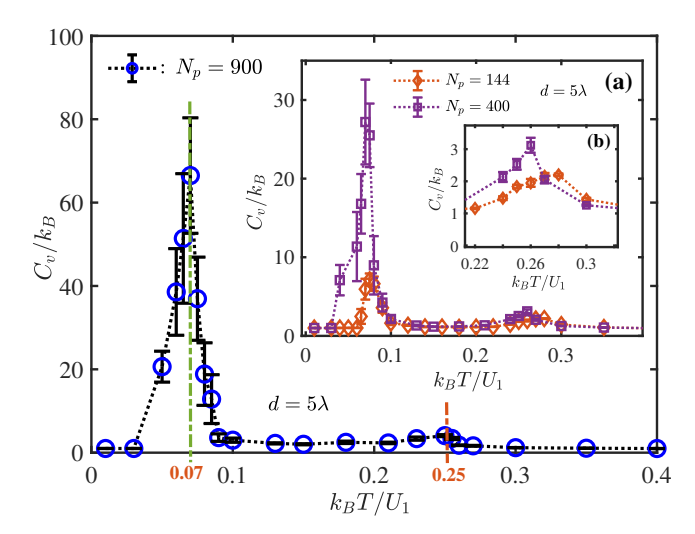


FIG. 2. Main plot: The variation of specific heat  $C_v$  (in units of  $k_B$ ) as a function of  $k_BT$  (in units of  $U_1=U_0\frac{e^{-5}}{5\lambda}$ ) at  $d=5\lambda$  for  $N_p=900$ . The  $C_v$  has two peaks, one at  $k_BT_{c1}=0$  $0.07 U_1$  and the other at  $k_B T_{c2} = 0.25 U_1$ . These two peaks correspond to the phase transitions from solid to hexatic and hexatic to modulated liquid phases. The inset plot (a) shows the variation of  $C_v$  for the other two smaller system sizes with  $N_p = 144$  and 400. For  $N_p = 144$ , the solid to hexatic transition happens at  $k_B T_{c1} = 0.075 U_1$  and the hexatic to liquid transition at  $k_B T_{c2} = 0.28 U_1$  Similarly, for  $N_p = 400$ , the solid to hexatic transition occurs at  $k_B T_{c1} = 0.07 U_1$  and the hexatic to liquid transition at  $k_B T_{c2} = 0.26 U_1$ . Inset plot (b) shows the enlarged portion of the hexatic-liquid transition for  $N_p = 144$  and  $N_p = 400$ . There is a clear shift in both the transition temperatures with system size as well as an increase in the  $C_v$  values at both transitions. Here, the error bars indicate the standard deviation of the mean, and the dotted lines shown are guides to the eye.

findings indicate that the intermediate phase is a hexatic phase, with no long-range translational order but with bond orientational order being present. The static structure factor for various phases is shown in Fig.5 and clearly indicates the solid, intermediate, and liquid phases at various temperatures. The change in the peak value of the structure factor corresponding to the reciprocal lattice vectors  $\mathbf{G_1}$  and  $\mathbf{G_2}$  with temperature is plotted in Fig.3 (see insets). These two display a smooth drop near the temperature corresponding to the loss of positional order, as in the case of the translational order parameter.

A finite-size scaling analysis of the peaks in specific heat  $C_v$  for  $d=5\lambda$  (see Fig.6) has been carried out in the system to confirm the nature of the phase transitions. As seen Fig.2, peaks in  $C_v$  become sharper when the size of the system is increased and the transition temperature reduces. The peak value of specific heat,  $C_{vm}$ , is found to scale as  $L^{\alpha/\nu}$ , where  $L=\sqrt{N_p}$ , at both the transitions. The scaling exponents for the solid-hexatic and the hexatic-liquid transitions are found to have values  $\alpha_1/\nu_1=2.34\pm0.10$  and  $\alpha_2/\nu_2=0.66\pm0.02$ , respectively. This analysis points again to the fact that the transitions

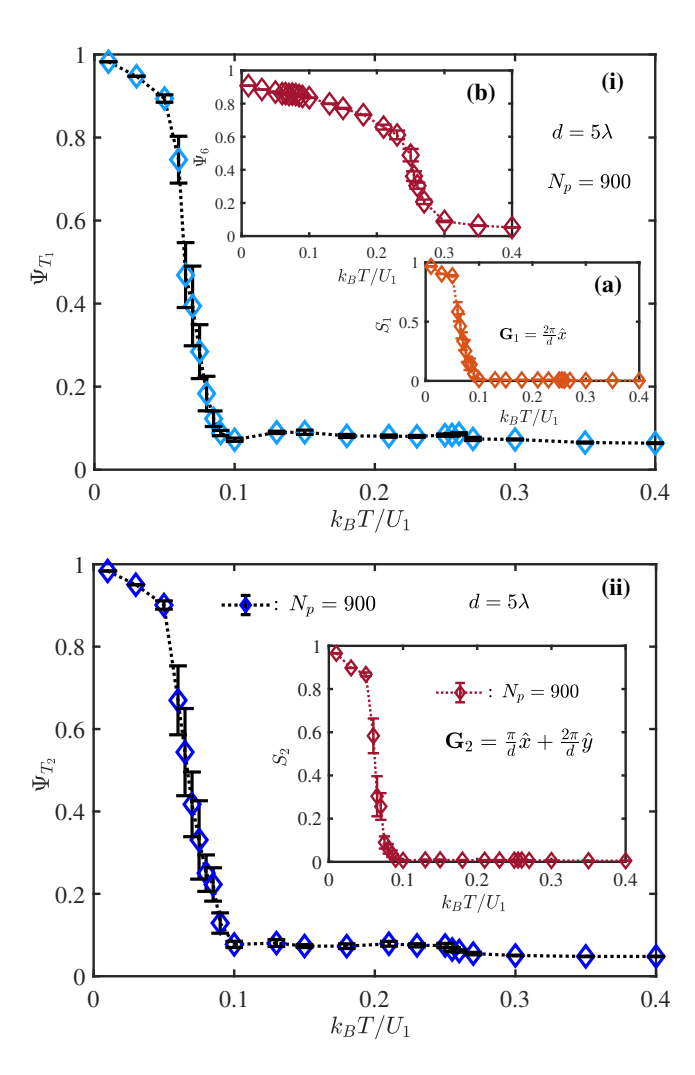


FIG. 3. (i) Variation of translational order parameter  $\Psi_{T1}$  corresponding to  $\mathbf{G_1}$  as a function of  $k_BT$  (in units of  $U_1=U_0\frac{e^{-5}}{5\lambda}$ ) for  $N_p=900$  at  $d=5\lambda$ . The corresponding structure factor  $S_1$  for  $\mathbf{G_1}$  is shown in the inset plot (a). Here, both  $\Psi_{T1}$  and  $S_1$  show a continuous drop around the transition temperature  $k_BT_{c1}$ . Inset plot (b) shows the variation of the orientational order parameter  $\Psi_6$  with  $k_BT$ . It has a continuous drop around the second transition temperature  $k_BT_{c2}$ . (ii) Variation of translational order parameter  $\Psi_{T2}$  as a function of  $k_BT$  for  $N_p=900$  at  $d=5\lambda$ . The corresponding variation of  $S_2$  for the reciprocal lattice vector  $\mathbf{G_2}$  is shown in the inset plot.  $\Psi_{T2}$  and  $S_2$  also drop continuously around the transition temperature  $k_BT_{c1}$ . The dotted line indicates the guide to the eye, and the error bars are the standard deviation of the mean.

observed in this case are second-order. In the KTHNY type of melting, one expects a peak in specific heat, but it is not expected to scale with system size. For example, an experimental study carried out on superparamagnetic polystyrene beads confined in 2D shows a single peak in specific heat  $C_v$  as a function of temperature [64]. The observed peak in  $C_v$  in the hexatic phase in that work indicates the maximum increase in the value of isolated

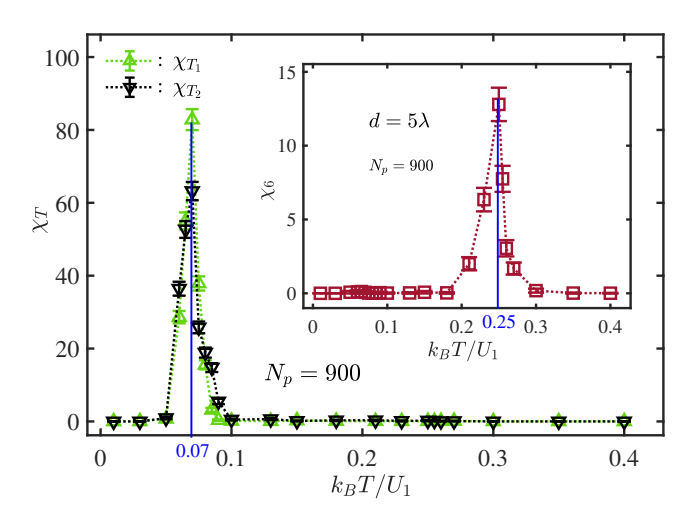


FIG. 4. Main plot: Variation of the translational susceptibilities  $\chi_{T1}$  and  $\chi_{T2}$  as a function of  $k_BT$  (in units of  $U_1 = U_0 \frac{e^{-5}}{5\lambda}$ ) for  $N_p = 900$  at  $d = 5\lambda$ . The inset plot shows the variation of orientational susceptibility  $\chi_6$  as a function of  $k_BT$ . Both the plots accurately locate the transition temperatures  $k_BT_{c1} = 0.07~U_1$  and  $k_BT_{c2} = 0.25~U_1$  marked by a solid blue line, using the peaks of  $\chi_T$ 's and  $\chi_6$ . Error bars represent the standard deviation of the mean, and the dotted lines indicate guides to the eye.

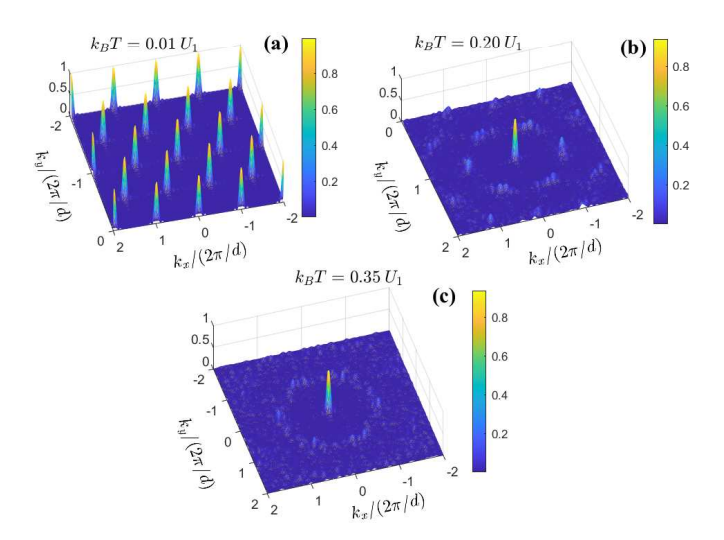


FIG. 5. Structure factor in different phases for the case  $d=5\lambda$ . (a) The partially pinned solid phase with true long-range positional and orientational orders at  $k_BT=0.01U_1$ . (b) The intermediate hexatic phase with short-range positional order and quasi-long-range orientational order at  $k_BT=0.20\ U_1$ . (c) The liquid phase with short-range positional and orientational orders at  $k_BT=0.35\ U_1$ .

# dislocations.

Since both transitions seen for  $d=5\lambda$  are found to be second-order, which is novel and contrary to what the KTHNY theory predicts, it would be interesting to look at the correlation functions and defect structure in

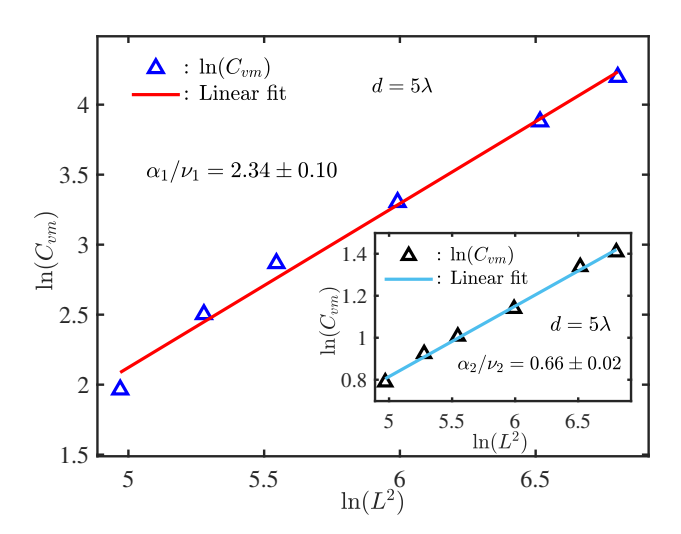


FIG. 6. Main plot: Scaling behavior of the first transition peak  $C_{vm}$  of the specific heat as a function of system size  $L^2$  in the log-log scale for  $d=5\lambda$ . The inset plot shows the scaling behavior of the second transition peak  $C_{vm}$  of the specific heat with system size  $L^2$  in the log-log scale for  $d=5\lambda$ . The scaling exponents are  $\alpha_1/\nu_1=2.34\pm0.10$  and  $\alpha_2/\nu_2=0.66\pm0.02$  respectively for the first and second transitions. The triangles in the plots represent simulation points, and the solid line indicates the corresponding linear fit.

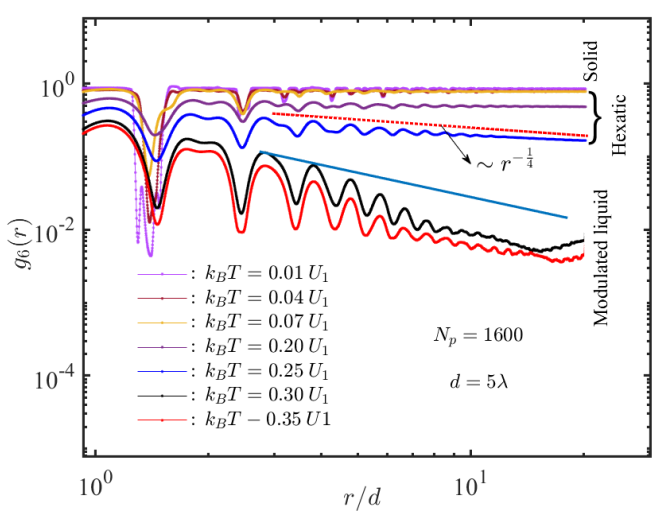


FIG. 7. The variation of orientational correlation function  $g_6(r)$  as a function of radial distance r in log-log scale for different values of  $k_BT$  for  $d=5\lambda$ , Np=1600. Three different phases are marked in the plot based on the nature of  $g_6(r)$ . In the hexatic phase, close to the hexatic-modulated liquid transition temperature, the correlation exponent  $\eta_6(T)$  has a value close to 1/4 (slope of the red dotted line is  $0.243\pm0.012$ ). This is aligned with the prediction of the KTHNY theory. In the modulated liquid phase,  $g_6$  has faster algebraic decay, indicating the absence of any long-range order.

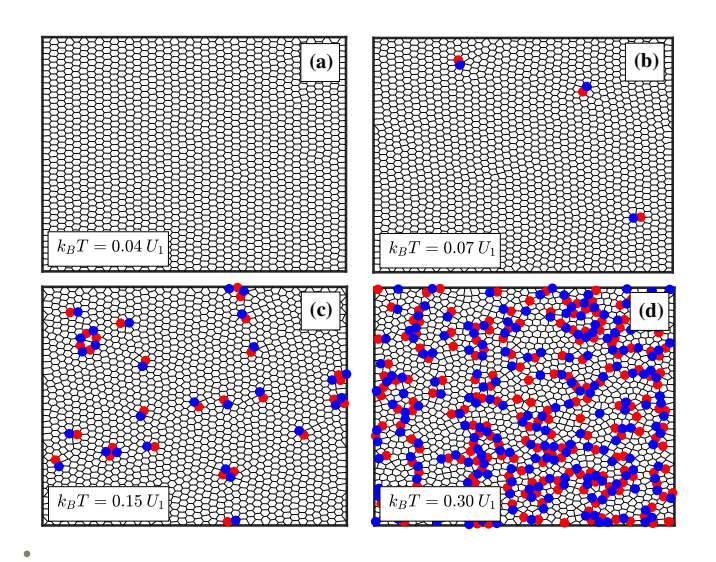


FIG. 8. Defect generation during the two-stage melting of the colloidal lattice ( $d=5\lambda$  and system size is  $N_p=900$ ). The red and blue dots indicate five-fold and seven-fold coordinated sites, respectively. The uncolored sites represent six-fold coordinated sites. (a) The crystalline phase with no defects at  $k_BT=0.04~U_1$ . (b) Unbound dislocations (or bound disclinations) are found close to the solid-hexatic transition point ( $k_BT=0.07~U_1$ ). (c) In the hexatic phase at  $k_BT=0.15~U_1$ , dislocations concentration increases considerably, and a fraction of them are found in bound form. A chain of defects formed by alternating coordination numbers can also be seen. (d) Defects proliferate in the liquid phase at  $k_BT=0.30~U_1$ , with many free disinclinations appearing along with chains of defects.

various phases for comparison. Orientational correlation function  $g_6(r)$  (calculated for  $N_p = 1600$ ) at different temperatures are shown Fig. 7.  $g_6(r)$  exhibits three distinct behaviors with r, depending on which of the three phases the system is in: solid, hexatic, or liquid. There is long-range order in the solid phase, algebraic decay in the hexatic phase, and exponential decay in the liquid phase. The nature of the exponent for the algebraic decay,  $\eta_6(T)$ , is such that it starts from low values at the transition point from solid to hexatic and reaches a maximum value close to  $\frac{1}{4}$  just before melting to the modulated liquid phase. One has an interesting situation wherein the system melts via two-stage melting as predicted by KTHNY theory, but the nature of the observed transitions is different from the KTHNY prediction. However, the orientational exponent  $\eta_6(T)$  at the hexatic-liquid transition temperature is found to be close to  $\frac{1}{4}$  (0.243 ± 0.012). This value of  $\eta_6(T)$  consistent with the value predicted by the KTHNY theory.

The results of the defect studies are shown in Fig.8. In the solid phase at low temperatures, the system is free of defects (Fig.8 (a)). This is expected as the system has true long-range order in this phase. Close to the solid to hexatic transition, free dislocations appear (Fig.8 (b)). In the hexatic regime, dislocations increase

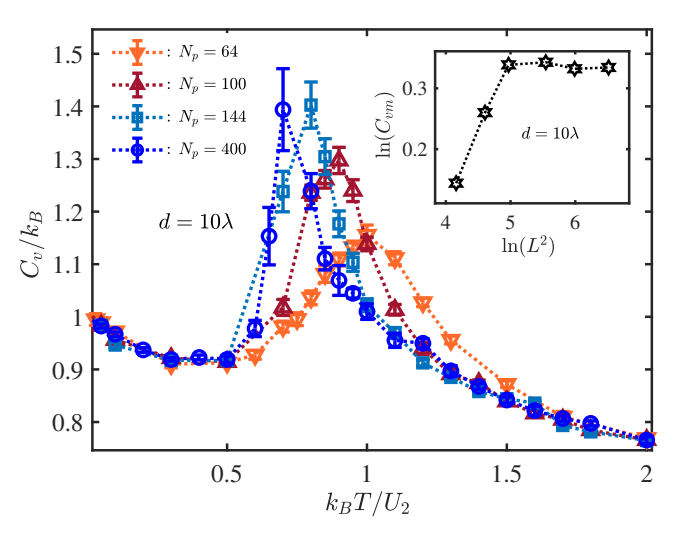


FIG. 9. The variation of specific heat  $C_v$  (in units of  $k_B$ ) as a function of  $k_BT$  (in units of  $U_2 = U_0 \frac{e^{-10}}{10\lambda}$ ) for  $N_p = 64,100,144$ , and 400 at  $d=10\lambda$ . A single peak in the specific heat is observed, and the location of the peak shifts to low temperatures with increasing system size. The inset plot shows the variation of the peak value of specific heat  $(C_{vm})$  as a function of system size  $L^2$  in the log-log scale for  $d=10\lambda$ . The dotted lines are guides to the eye, and the error bars are the standard deviation of the mean.

with temperature, some of which tend to form bound pairs, but many remain unbound (Fig.8 (c)). The unbound dislocations (or bound disclinations) are the reason for the loss of long-range bond orientational order in this phase. In the modulated liquid phase, the defect concentration is high, and seems to have a combination of free disclinations, a chain of defects, free dislocations, and a few bound dislocations (Fig. 8 (d)). The defect structure study shows that though there are similarities between the behavior observed and the KTHNY predictions for the homogeneous case, there are crucial differences. The intermediate phase observed is similar to the hexatic phase, borne out by both the defect structure and the  $g_6(r)$  behavior. The transition to the modulated liquid phase seems to be driven by bound disclinations unbinding. The low-temperature crystal phase is free from defects, and its melting to the hexatic phase is via a conventional, symmetry-breaking second-order transition.

To explore the effect of the substrate lattice parameter, d, on phases and phase transitions, simulations were carried out for  $d=10\lambda$  with the filling fraction kept at n=1. For  $d=10\lambda$  and  $A_s=10^{-4}$ , the ground state is found to be the partially pinned solid in this case as well, with an equal separation distance of  $\approx 0.23 \, d$  from the minima on either side of the square cell. This phase has true long-range translational and orientational orders (See Fig.1). This phase undergoes a transition to a modulated liquid phase as the temperature is increased. The variation of specific heat  $C_v$  as a function of  $k_BT$ 

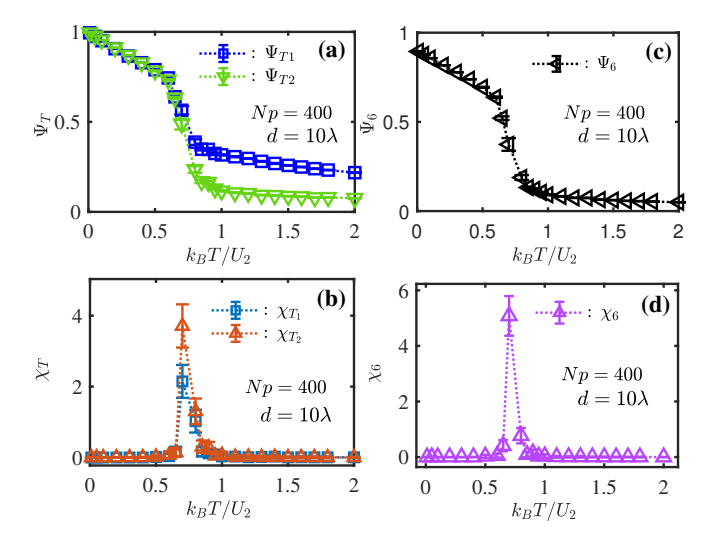


FIG. 10. (a) Variation of the translational order parameters  $\Psi_{T1}$  (corresponding to  $\mathbf{G_1}$ ) and  $\Psi_{T2}$  (corresponding to  $\mathbf{G_2}$ ) as a function of  $k_BT$  (in units of  $U_2 = U_0 \frac{e^{-10}}{10\lambda}$ ) for  $N_p = 400$  at  $d = 10\lambda$ . (b) The corresponding susceptibilities  $(\chi_{T_1} \& \chi_{T_2})$ . Plots (c) & (d) show the variation of the orientational order parameter  $\Psi_6$  and its corresponding  $\chi_6$  as a function of  $k_BT$ . The behavior seen clearly indicates a single transition at which the solid melts to a modulated liquid. Here, symbols are the simulation points, and the dotted lines are guides to the eye. Error bars shown in the plots are the standard deviation of the mean.

for Np=400,144,100 and 100 at  $d=10\lambda$  is shown in Fig.9. A single peak in  $C_v$  is observed. The location of the peak saturates to a value close to  $k_BT_c=0.7~U_2$  as the system size is increased. The locations of the peak in  $C_v$  for the system sizes  $N_p=400,144,100$  and 64 are respectively at  $k_BT_c=0.7~U_2,~0.8~U_2,~0.9~U_2$  and  $0.95~U_2,$  where  $U_2=U_0~\frac{e^{-10}}{10\lambda}$ , is the energy scale of inter-particle interaction. The peak value of  $C_v$  is seen to saturate with the size of the system (see the inset of Fig.9).

The translational  $(\Psi_T)$  and the bond orientational  $(\Psi_6)$  order parameters show a continuous drop near the transition temperature. The order parameters for  $N_p =$ 400 at  $d=10\lambda$  are shown in Fig.10. The translational order parameter  $(\Psi_T)$  is computed for the two smallest reciprocal lattice vectors  $\mathbf{G_1} = \frac{2\pi}{d}\hat{x}$  and  $\mathbf{G_2} = \frac{\pi}{d}\hat{x} + \frac{2\pi}{d}\hat{y}$  of the partially pinned solid. Since the order parameter calculations are inconclusive in locating the transition points, the susceptibility calculation has been carried out from the fluctuations of the order parameters to locate the points where the phase transition happens. The peak in susceptibilities,  $\chi_6$ ,  $\chi_{T_1}$ , and  $\chi_{T_2}$ , is found to be located at the same temperature to within the resolution that simulations could provide. This temperature coincides with the peak in  $C_v$  for the large system size limit. These results point to a scenario where the low-temperature solid phase transitions to a modulated liquid via a continuous crossover. This result is different from the observations in the previous work on the vortex lattice melting [61], where a continuous transition was observed.

To address the question of how the nature of the transition changes from two-stage melting to a single crossover, the transitions have been studied for a range of values of d with the value of  $A_s$  fixed at  $10^{-4}$ . We find that for the value of  $d \lesssim 9\lambda$ , there are two second-order transitions similar to  $d=5\lambda$  case presented above. These two transitions come close and merge to a single crossover for  $d\approx 9\lambda$ . This seems to indicate that for smaller values of d, the system behaves similarly to the homogeneous system, which also exhibits two-stage melting. In fact, it can be argued that as d is decreased, the effect of the substrate becomes weaker as follows. The interaction of a colloidal particle with a pinned particle located at the corner of the square cell is given by

$$U^{cp} = A_s U_0 \frac{e^{-\frac{d}{\sqrt{2}\lambda}}}{\frac{d}{\sqrt{2}}} \tag{9}$$

Similarly, the interaction between two colloidal particles separated by a lattice spacing, d, is given by

$$U^{cc} = U_0 \, \frac{e^{-\frac{d}{\lambda}}}{d} \tag{10}$$

The ratio  $\frac{U^{cp}}{U^{cc}}$  gives an estimate of the strength of the substrate relative to the inter-particle interaction and is given by

$$\frac{U^{cp}}{U^{cc}} = \sqrt{2} A_s e^{d(1 - \frac{1}{\sqrt{2}})} . {11}$$

This ratio decreases with d, indicating the effect of the substrate is reduced at smaller d values. Consistent with this observation, we find that for large enough d, the ground state has square symmetry, implying that the substrate dictates the symmetry of the ground state.

To cross-check the above hypothesis, simulations were done with d kept fixed at  $5\lambda$  and  $A_s$  varied. It is found that for larger values of  $A_s$  ( $A_s \gtrsim 0.001$ ), a single transition is observed where both  $\psi_T$  and  $\psi_6$  go to zero simultaneously. The specific heat shows a peak but shows no scaling behavior with system size, implying a crossover. For large enough values of  $A_s$  ( $A_s \gtrsim 0.1$ ), the ground state has square symmetry and no transition is observed when the temperature is increased. These results are consistent with the results discussed above with varying d values. In the limit when the substrate strength,  $A_s$ goes to zero, our results match the two-stage melting of the homogeneous case, observed by Yong Chen et al. [51] in their studies. The results based on the order parameter, susceptibility, and orientational correlation function calculations show agreement with the KTHNY theory predictions, but the observed defect structure was complex compared to the predictions of the KTHNY theory.

#### IV. SUMMARY

The equilibrium phase behavior of a colloidal lattice in a 2D periodic substrate of square symmetry has been studied using the Monte-Carlo simulation for filling fraction n = 1. Earlier studies on similar systems have shown that when the particle-substrate interaction becomes comparable to the inter-particle interaction, the system forms a partially pinned structure with only one of the basic periodicities associated with the substrate present. [60, 61, 65]. This phase melts into a modulated liquid phase via a single second-order transition. The focus of the present work is to study how the colloidal system behaves as the substrate parameter, d, is varied with the screening length  $\lambda$  fixed. The key findings of this study are the following:

- (i) For values of  $d \gtrsim 9\lambda$ , there is a single transition or crossover from a solid to a modulated liquid. This is unlike what is observed in the hard-sphere and vortex systems.
- (ii) For lower values of d, there is a two-stage melting from the low-temperature crystal to a modulated liquid, with an intermediate hexatic phase being present. Both these transitions are found to be second-order in nature. These transitions are not of Ising-type as is predicted by Nelson et al. [56].
- (iii) On increasing the substrate strength for a fixed value of d, the two-stage melting is replaced by a single crossover from solid to modulated liquid, much like the observation in point (i) above. Both these behaviors can be attributed to the increasing influence of the lattice as d or  $A_s$  is increased.
- (iv) If the substrate strength is too strong (for example,  $A_s > 0.1$  for  $d = 5\lambda$ ), the ground state has square symmetry, and no transition is observed with increasing temperature.
- (v) The results from the defect study confirm the presence of an intermediate hexatic phase with free

dislocations.

The results obtained in this work give insights into the problem of the melting transitions of a 2D solid when the strength of the underlying substrate is weak for filling fraction n = 1. Even though the system undergoes two continuous transitions for low substrate strengths, these transitions are different from the continuous transitions predicted by KTHNY theory of 2D melting. During the transition from the solid to the hexatic phase, the system loses long-range positional order. In the second transition, the quasi-long-range orientational order is lost. Though this transition is not a KT-type transition, the exponent  $\eta_6(T)$  corresponding to the algebraic decay of orientational correlation function is close to the value of  $\frac{1}{4}$  as predicted by the KTHNY theory. At both transitions  $C_v$  shows clear scaling with system size, confirming that the transitions are of second order. Another related 2D system where multiple transitions have been observed is the generalized XY model with higher order nematic-like couplings [66].

The focus of the current study has been to understand the different phases and phase transitions of the colloidal system in a square periodic substrate for the case of filling, n = 1. Both the substrate strength,  $A_s$ , and lattice parameter, d, have been varied to see their influence on the phases. A natural extension of the work would be to study the system for other fillings. The observation of two continuous second-order transitions in a 2D particle system is novel. Its possible connection to the generalized XY model, where multiple continuous transitions have been seen, is intriguing. It is to be noted here that even though the current work is carried out for colloidal systems, the physics behind the phenomenon observed in this work would be relevant for other systems like superconducting vortices, particles adsorbed on a metallic surface, and other relevant systems.

### ACKNOWLEDGMENTS

The authors would like to acknowledge the financial support under the DST-SERB Grant No: CRG/2020/003646.

<sup>[2]</sup> J. Μ. Kosterlitz and D. J. Thouless, Journal of Physics C: Solid State Physics 6, 1181 (1973).

<sup>[3]</sup> J. Μ. Kosterlitz and D. Thouless, Journal of Physics C: Solid State Physics 5, L124 (1972)

<sup>[4]</sup> B. Ι. Halperin and D. R. Nelson, Phys. Rev. Lett. 41, 121 (1978).

<sup>[5]</sup> D. R. Nelson and В. I. Halperin, Phys. Rev. B 19, 2457 (1979).

<sup>[6]</sup> A. P. Young, Phys. Rev. B 19, 1855 (1979).

<sup>[1]</sup> N. D. Mermin, Journal of Mathematical Physics 8, 1061 (1967) A. Widom, J. R. Owers-Bradley, and M. G. Richards, Phys. Rev. Lett. **43**, 1340 (1979).

<sup>[8]</sup> D. E. Angelescu, C. K. Harrison, M. L. Trawick, R. A. Register, and P. M. Chaikin, Phys. Rev. Lett. 95, 025702 (2005).

<sup>[9]</sup> A. V. Petukhov, D. van der Beek, R. P. A. Dullens, I. P. Dolbnya, G. J. Vroege, and H. N. W. Lekkerkerker, Phys. Rev. Lett. **95**, 077801 (2005).

<sup>[10]</sup> S. Deutschländer, T. Horn, H. Löwen, G. Maret, and P. Keim, Phys. Rev. Lett. 111, 098301 (2013).

- [11] Y. Han, N. Y. Ha, A. M. Alsayed, and A. G. Yodh, Phys. Rev. E 77, 041406 (2008).
- [12] T. Horn, S. Deutschländer, H. Löwen, G. Maret, and P. Keim, Phys. Rev. E 88, 062305 (2013).
- [13] H. H. von Grünberg, P. Keim, K. Zahn, and G. Maret, Phys. Rev. Lett. 93, 255703 (2004).
- [14] R. E. Kusner, J. A. Mann, J. Kerins, and A. J. Dahm, Phys. Rev. Lett. 73, 3113 (1994).
- [15] K. Zahn and G. Maret, Phys. Rev. Lett. 85, 3656 (2000).
- [16] Y. Peng, Z. Wang, A. M. Alsayed, A. G. Yodh, and Y. Han, Phys. Rev. Lett. 104, 205703 (2010).
- [17] T. F. Rosenbaum, S. E. Nagler, P. M. Horn, and R. Clarke, Phys. Rev. Lett. 50, 1791 (1983).
- [18] J. Schockmel, E. Mersch, N. Vandewalle, and G. Lumay, Phys. Rev. E 87, 062201 (2013).
- [19] P. Keim, G. Maret, and H. H. von Grünberg, Phys. Rev. E 75, 031402 (2007).
- [20] W. Brinkman, D. S. Fisher, and D. Moncton, Science 217, 693 (1982).
- [21] K. Zahn, R. Lenke, and G. Maret, Phys. Rev. Lett. 82, 2721 (1999).
- [22] D. S. Fisher, B. I. Halperin, and R. Morf, Phys. Rev. B 20, 4692 (1979).
- [23] T. V. Ramakrishnan, Phys. Rev. Lett. 48, 541 (1982).
- [24] S. T. Chui, Phys. Rev. Lett. 48, 933 (1982).
- [25] H. Kleinert, Physics Letters A 95, 381 (1983).
- [26] H. Kleinert, Physics Letters A 130, 443 (1988).
- [27] H. Kleinert, Physics Letters A 136, 468 (1989).
- [28] D. Frenkel and J. P. McTague, Phys. Rev. Lett. 42, 1632 (1979).
- [29] D. E. Dudalov, Y. D. Fomin, E. N. Tsiok, and V. N. Ryzhov, Phys. Rev. Lett. 112, 157803 (2014).
- [30] E. P. Bernard and W. Krauth, Phys. Rev. Lett. 107, 155704 (2011).
- [31] S. Z. Lin, B. Zheng, and S. Trimper, Phys. Rev. E **73**, 066106 (2006).
- [32] S. Prestipino, F. Saija, and P. V. Giaquinta, Phys. Rev. Lett. 106, 235701 (2011).
- [33] Y. Saito, Phys. Rev. Lett. 48, 1114 (1982).
- [34] K. J. Strandburg, J. A. Zollweg, and G. V. Chester, Phys. Rev. B 30, 2755 (1984).
- [35] K. J. Strandburg, S. A. Solla, and G. V. Chester, Phys. Rev. B 28, 2717 (1983).
- [36] J. Tobochnik and G. V. Chester, Phys. Rev. B 25, 6778 (1982).
- [37] C. Udink and J. van der Elsken, Phys. Rev. B 35, 279 (1987).
- [38] H. Weber, D. Marx, and K. Binder, Phys. Rev. B 51, 14636 (1995).

- [39] K. Wierschem and E. Manousakis, Phys. Rev. B 83, 214108 (2011).
- [40] N. Gribova, A. Arnold, T. Schilling, and C. Holm, The Journal of chemical physics 135 (2011).
- [41] F. F. Abraham, Phys. Rev. Lett. 44, 463 (1980).
- [42] S. Toxvaerd, Phys. Rev. Lett. 44, 1002 (1980).
- [43] H. Shiba, A. Onuki, and T. Araki, Europhysics Letters 86, 66004 (2009).
- [44] K. Chen, T. Kaplan, and M. Mostoller, Phys. Rev. Lett. 74, 4019 (1995).
- [45] A. H. Marcus and S. A. Rice, Phys. Rev. Lett. 77, 2577 (1996).
- [46] D. Frenkel and J. P. McTague, Phys. Rev. Lett. 42, 1632 (1979).
- [47] F. L. Somer, G. S. Canright, T. Kaplan, K. Chen, and M. Mostoller, Phys. Rev. Lett. 79, 3431 (1997).
- [48] J. A. Zollweg and G. V. Chester Phys. Rev. B 46, 11186 (1992).
- [49] J. F. Fernández, J. J. Alonso, and J. Stankiewicz, Phys. Rev. Lett. 75, 3477 (1995).
- [50] A. Jaster, Phys. Rev. E **59**, 2594 (1999).
- [51] W.-K. Qi, Z. Wang, Y. Han, and Y. Chen, The Journal of chemical physics 133 (2010).
- [52] Q.-H. Wei, C. Bechinger, D. Rudhardt, and P. Leiderer, Phys. Rev. Lett. 81, 2606 (1998).
- [53] L. Radzihovsky, E. Frey, and D. R. Nelson, Phys. Rev. E 63, 031503 (2001).
- [54] C. Bechinger, M. Brunner, and P. Leiderer, Phys. Rev. Lett. 86, 930 (2001).
- [55] W. Strepp, S. Sengupta, and P. Nielaba, Phys. Rev. E 63, 046106 (2001).
- [56] D. R. Nelson and B. I. Halperin, Phys. Rev. B 19, 2457 (1979).
- [57] N. Greiser, G. A. Held, R. Frahm, R. L. Greene, P. M. Horn, and R. M. Suter, Phys. Rev. Lett. 59, 1706 (1987).
- [58] Q. M. Zhang and J. Z. Larese, Phys. Rev. B 43, 938 (1991).
- [59] R. E. Ecke and J. G. Dash, Phys. Rev. B 28, 3738 (1983).
- [60] T. Neuhaus, M. Marechal, M. Schmiedeberg, and H. Löwen, Phys. Rev. Lett. 110, 118301 (2013).
- [61] T. Joseph and C. Dasgupta Phys. Rev. B 66, 212506 (2002).
- [62] R. Zangi and S. A. Rice, Phys. Rev. E 58, 7529 (1998).
- [63] Z. Wang, A. M. Alsayed, A. G. Yodh, and Y. Han, The Journal of chemical physics 132 (2010).
- [64] S. Deutschländer, A. M. Puertas, G. Maret, and P. Keim, Phys. Rev. Lett. 113, 127801 (2014).
- [65] T. Joseph, Physica A: Statistical Mechanics and its Applications 556
- [66] M. Žukovič, Entropy **26**, 893 (2024).